



HAL
open science

The lacquer crafting of Ba state: Insights from a Warring States lacquer scabbard excavated from Lijiaba site (Chongqing, southwest China)

Bin Han, Xiaopan Fan, Yun Chen, Jie Gao, Michel Sablier

► To cite this version:

Bin Han, Xiaopan Fan, Yun Chen, Jie Gao, Michel Sablier. The lacquer crafting of Ba state: Insights from a Warring States lacquer scabbard excavated from Lijiaba site (Chongqing, southwest China). *Journal of Archaeological Science: Reports*, 2022, 42, pp.103416. 10.1016/j.jasrep.2022.103416 . hal-03788584

HAL Id: hal-03788584

<https://hal.science/hal-03788584>

Submitted on 10 Oct 2022

HAL is a multi-disciplinary open access archive for the deposit and dissemination of scientific research documents, whether they are published or not. The documents may come from teaching and research institutions in France or abroad, or from public or private research centers.

L'archive ouverte pluridisciplinaire **HAL**, est destinée au dépôt et à la diffusion de documents scientifiques de niveau recherche, publiés ou non, émanant des établissements d'enseignement et de recherche français ou étrangers, des laboratoires publics ou privés.

1 **The lacquer crafting of *Ba* state: insights from a Warring States lacquer**
2 **scabbard excavated from Lijiaba site (Chongqing, southwest China)**

3
4 Bin Han^a, Xiaopan Fan^{b*}, Yun Chen^c, Jie Gao^d, Michel Sablier^{e*},

5 ^a Department of Archaeology and Anthropology, School of Humanities, University of
6 Chinese Academy of Sciences, 100049 Beijing, China

7 ^b History and Social Work College, Chongqing Normal University, 401331
8 Chongqing, China

9 ^c Yunyang Museum, 404500 Chongqing, China

10 ^d Shimadzu (China) Co. LTD, 100020 Beijing, China

11 ^e Centre de Recherche sur la Conservation (CRC, USR 3224), Muséum national
12 d'Histoire naturelle, Ministère de la Culture, CNRS, 75005 Paris, France

13
14 *corresponding authors: fxiaopan@163.com (X. Fan); michel.sablier@mnhn.fr (M.
15 Sablier)

16 **Abstract:** The lacquer scabbard of a bronze sword dating from the Warring States
17 (476-221 BC) and excavated from a *Ba* tomb of the Lijiaba site (Chongqing,
18 southwest China) was characterized by a multidisciplinary approach including
19 microscopy, scanning electron microscopy-energy dispersive X-ray spectrometry
20 (SEM-EDS), Raman spectroscopy and pyrolysis-gas chromatography/mass
21 spectrometry (Py-GC/MS). Pyrolysis-comprehensive two-dimensional gas
22 chromatography/mass spectrometry (Py-GCxGC/MS) has been applied for the first
23 time for the characterization of a valuable archaeological lacquer sample confirming
24 the benefits of this technique for the description of the ingredients used in the
25 formulation of the lacquer coating. Besides, the analytical results also showed that, in
26 accordance with what is suspected from the lacquer technique employed at this period,
27 two lacquer film layers and a bone-derived ground layer were present as confirmed by
28 the characterization of hydroxyapatite particles ($\text{Ca}_5(\text{PO}_4)_3\text{OH}$) of different sizes.
29 Py-GC/MS analysis allowed identification of the origin of the scabbard lacquer as a
30 *Toxicodendron vernicifluum* lacquer and detection of potential drying oil markers,
31 while Py-GCxGC/MS analysis revealed the presence of a series of polyaromatic
32 hydrocarbons (PAHs) compounds non-characterizable by 1D GC/MS analysis. This
33 latter observation highlights the use of soot attributed to a plant origin in conjunction
34 with bone for the manufacture and coloring of the lacquers.

35 **Key words:** *Ba* ethnic group, Lijiaba site, lacquer scabbard, Asian lacquer,
36 *Toxicodendron vernicifluum*, Py-GCxGC/MS, PAHs characterization

37 1. Introduction

38 Lacquer is a natural product which is polymerized by laccase enzyme and has been
39 used as coating materials for wooden crafts, ceramics, leather and metal artifacts since
40 the Neolithic period (Zhai et al., 2021). Lacquer sap usually contains urushiol, plant
41 gum, laccase, nitrogen substance, and water. Different lacquer trees, depending on
42 their locations of growth, have been traditionally used for lacquer making in the
43 countries where lacquer artworks have been developed (Lu et al., 2012). Globally, the
44 Asian lacquer reported as *shengqi* (in China) and *urushi* (in Japan) is a sap collected
45 from lacquer trees of the *Toxicodendron vernicifluum* (Stokes) F. A. Barkley species,
46 for which the principal component is urushiol (C15 unsaturated hydrocarbon chains at
47 the 3-position of the catechol ring). Vietnam's and Taiwan region's lacquer consists
48 in a sap exuded from lacquer trees of the *Toxicodendron succedaneum* (L) Kuntze
49 species, where the principal component is laccol (C17 unsaturated hydrocarbon chain
50 at the 3-position of the catechol ring). In some part of southern China, *Toxicodendron*
51 *succedaneum* has also been reported as lacquer sap origins (e.g., in the Guangxi
52 province that is close to Vietnam) (Wan et al., 2007; Heginbotham et al., 2016).
53 Myanmar, Laos, Cambodia, and Thailand lacquers consist of a sap exuded from *Gluta*
54 *usitata* (Wall.) Ding Hou lacquer tree species, and their principal component is thitsiol
55 (4- and/or 3-substituted catechol derivatives with 17 carbon chains) (Ma et al., 2014).
56 The polyhydroxy phenols (urushiol, laccol, thitsiol) are the main compositions of
57 lacquer and their chemical differences can be intentionally used to differentiate the
58 origin of lacquer sample.

59 As a cross-linked polymer, Lacquer film is insoluble in most solvents and only a few
60 analytical techniques are appropriate for its analysis. Pyrolysis-gas
61 chromatography/mass spectrometry (Py-GC/MS) is effective and mostly used for
62 lacquer film analysis due to its minimum quantity required, easy sample preparation
63 and effective in lacquer origin tracing. Typical pyrolysis products issued from lacquer
64 samples are principally alkanes, alkenes, alkylbenzenes, alkylphenols and
65 alkylcatechols products (Lu et al., 2012 and references cited therein). If different
66 patterns in the resulting chromatograms can be observed depending on the pyrolysis
67 system used for lacquer analysis (Le Hô et al., 2012), basically, these products are still
68 present and represent the usual markers of origin for the characterization of lacquer
69 samples (Ma et al., 2014). Consequently, by using an extracted ion chromatogram
70 procedure for the treatment of mass spectrometry data, it is possible to identify the
71 components of the lacquer saps to determine the origin of the lacquer samples.

72 Although lacquer has a long history in China (Zhai et al., 2021) and some researches
73 have disclosed on the ancient lacquer in other areas in China (Jin et al., 2012; Wei et

74 al., 2011; Jin et al., 2017; Hao et al., 2017; Fu et al., 2020; Zheng et al., 2020; Xiao et
75 al., 2020), there is no specific research dedicated to the lacquer craft of marginal area
76 (e.g., the *Ba* State in the southwest part of China). Furthermore, the beneficial of
77 GCxGC/MS separation of complex additives in lacquer crafting has not yet been
78 explored in archaeological samples except our previous work on pure modern lacquer
79 film (Okamoto et al., 2018).

80 *Ba* group was an ethnic group living in southwest China, upper stream of the Yangtze
81 River during a period extending from the Shang Dynasty to the Qin Dynasty (ca.1600
82 BC-221 BC). The associated *Ba* State developed a stronger power in the Spring and
83 Autumn period (770-476 BC) which continued during the Warring States (476-221
84 BC). *Ba* State had close cultural and economic exchanges as well as military conflicts
85 with its neighboring *Chu* State (Bai, 2020). Some typical sites of *Ba* culture in the
86 Chongqing area such as the Shuangyantang site in Wushan, the Lijiaba site in
87 Yunyang (Fan and Freestone, 2017), the Yujiaba site in Kai county (Fan et al, 2020),
88 and the Xiaotianxi site in Fuling were unearthed through archaeological discoveries.
89 Among them, the Lijiaba site (Fig.1), located on the eastern bank of the Pengxi river
90 (a branch of the Yangtze River) is known as the regional center of *Ba* state in the
91 Pengxi river basin. Lijiaba site is of utmost importance for the research of *Ba* culture
92 as well as for the findings of evidence of exchanges of these *Ba* people with other
93 cultures that are contemporary to its development.

94 **Figure 1**

95 In order to increase our knowledge on the lacquer crafts of the *Ba* ethnic group, the
96 lacquer film sample from the scabbard of a bronze sword (03YLM11:10) dated to the
97 Warring States period were studied by a multidisciplinary approach including
98 microscopy, scanning electron microscopy-energy dispersive X-ray spectrometers
99 (SEM-EDS), Raman spectroscopy, pyrolysis coupled to gas chromatography/mass
100 spectrometry (Py-GC/MS) and coupled to comprehensive two-dimensional gas
101 chromatography/mass spectrometry (Py-GCxGC/MS). As a result, new elements for a
102 complete description of the lacquer coating of this representative artifact of the *Ba*
103 ethnic group were obtained.

104

105 **2. Experimental**

106 **2.1 The archaeological background and materials**

107 The Lijiaba site is situated in the Qingshu village (Yunyang county), Chongqing,
108 southwest China (31°6'15"N, 108°41'E) (Fig.1). It was discovered in 1987 and
109 archaeological survey and tentative excavations were carried out between 1992 and
110 1995, prior to regular excavations started in 1997. The collected material remains
111 from this site suggested that it was inhabited during a long period spanning from the
112 Shang-Zhou Dynasty to the Six Dynasties (ca.1600 BC–ca.600 AD) (Chongqing 2001,
113 2003). The exceptional nature of the findings conducted in the selection of the site as
114 one of the *Top Ten Archaeological Discoveries in China*. Numerous tombs from the
115 Eastern Zhou Dynasty (770-221 BC), which includes the Spring and Autumn period
116 and the Warring States period were excavated there.

117 **Figure 2**

118 Besides bronze (Fan and Freestone 2017) and pottery artefacts (Wu et al. 2013),
119 lacquer film marks and lacquer objects were also found in Lijiaba site (Chongqing.
120 2001, 2003). The lacquer film residue studied in this paper was found on the scabbard
121 of the bronze sword in the tomb 2003YLM11 (archaeological number 03YLM11:10,
122 Fig.2). The tomb was located in the center of area III of Lijiaba site which is a
123 rectangular earthen pit tomb and filled with a lot of green paste mud (Fig.2). Other
124 archaeological objects unearthed with the bronze sword consist in ceramic and bronze
125 artifacts shown in Fig.2.

126 **Figure 3**

127 A relatively small surface of lacquer coating was preserved intact on the surface of the
128 scabbard of the bronze sword. Some small lacquer fragments spontaneously detached
129 from the scabbard were chosen for analysis since they provided lacquer samples of
130 interest in avoiding further sampling, which could be prejudicial for the integrity of
131 the scabbard, already noticeably damaged.

132 **2.2 Microscope observation**

133 Digital microscopy (VHX-5000 Keyence) used in reflection mode permitted to reveal
134 the surface profiles of lacquer samples. The lacquer sample was mounted in epoxy
135 resin at room temperature and polished. And the sample was coated with carbon for
136 SEM analysis. A FEI-Quanta 200 environmental scanning electron microscope (SEM)
137 equipped with an X-ray energy dispersive spectroscopy (EDS) system was utilized to
138 observe morphologies of the samples in high-vacuum mode applying an accelerating
139 voltage of approximately 20 kV.

140 **2.3 Raman spectroscopy**

141 Raman spectra of the sample were recorded at room temperature with a Renishaw
142 inVia Raman microscope system from 3500 to 50 cm^{-1} in extensive mode with a laser
143 wavelength of 532 nm and 50L \times objective lens. Laser power was set for emission at 1
144 percent power, which corresponds to ca. 0.5 mW with an integration time of 10 s. The
145 number of accumulations was fixed from 1 to 10.

146 **2.4 Py-GC/MS Analysis**

147 The Py-GC/MS system consisted of a vertical micro-furnace pyrolyzer PY-2020iD
148 (Frontier Lab, Fukushima, Japan) fitted to a Shimadzu QP2010Plus GC/MS instrument
149 (Shimadzu, Champs-sur-Marne, France). The mass of samples used for analysis lies
150 between 100-130 μg . The samples investigated by Py-GC/MS were cut with a scalpel
151 in tiny pieces after a cleaning and polishing step to eliminate dusts and trace of soil
152 contaminants under binocular magnifier. The state of the archaeological samples
153 permits with difficulty to separate properly the layers of lacquer. Consequently,
154 analysis was conducted on samples presenting the whole stratigraphy of the lacquer's
155 coatings, namely the layers described in section 3.1 below.

156 The conditions of analysis have been described elsewhere (Avataneo and Sablier,
157 2017). Briefly, the sample was introduced into the micro-furnace at 500 $^{\circ}\text{C}$;
158 chromatographic separation was conducted on an apolar fused silica capillary column 5%
159 phenyl-95% dimethyl polysiloxane (30 m length, 0.25 mm inner diameter, 0.25 μm
160 film thickness) with a the following oven temperature program: 2 min at 40 $^{\circ}\text{C}$,
161 ramping at 12 $^{\circ}\text{C min}^{-1}$ to 325 $^{\circ}\text{C}$, plateau at 325 $^{\circ}\text{C}$ for 10 min. The same experimental
162 conditions were applied for thermally-assisted hydrolysis and methylation (THM)
163 Py-GC/MS (Challinor, 2001). Only a volume of 3-5 μL of tetramethyl ammonium
164 hydroxide (25% in methanol) was added to the sample in the sample cup before its
165 introduction in the micro-furnace. The scan range of the mass spectrometer was set
166 from 40 to 500 u, operated at 5000 u. s^{-1} , and ionization was performed by electron
167 ionization at 70 eV. Identification of pyrolysis products was obtained by comparison of
168 their mass spectra with mass spectra of the NIST library (NIST, 2011) and by
169 interpreting the main fragmentations observed.

170 **2.5 Py-GCxGC/MS Analysis**

171 The Py-GCxGC/MS system consisted of a vertical microfurnace pyrolyzer PY-3030D
172 (Frontier Lab, Fukushima, Japan) fitted to a Shimadzu QP2010-Ultra mass
173 spectrometer (Shimadzu, Champs-sur-Marne, France) equipped with a two-stage
174 thermal modulator ZX 2 (Zoex, Houston, TX, USA). Quantities of lacquer sample
175 analyzed were about 50 μg , weighed with a microbalance (XP2U Ultra Micro
176 Balance, Mettler Toledo, Viroflay, France).

177 The GCxGC chromatography system consisted in an apolar capillary column
178 OPTIMA-5HT (30 m × 0.25 mm I.D., 0.25 μm film thickness, Macherey-Nagel,
179 Hoerd, France) in the first-dimension, and a moderate polar column Zebron ZB-50
180 (2.8 m × 0.1 mm I.D., 0.1 μm film thickness, Phenomenex, Le Pecq, France) in the
181 second-dimension and for the loop modulator system. The separation was carried out
182 in a constant pressure mode (300 kPa). The ZX 2 two-stage thermal modulator
183 operated a cooled air jet at −94°C, modulated with a pulsed hot air jet at a modulation
184 period of 9 s, and a programmed hot pulse duration of 0.350 s. Details for the analysis
185 have been reported previously (Okamoto et al, 2018), and consists briefly of an oven
186 temperature program initially held 5 min at 70°C, and increased at 3°C/min to 300°C,
187 where it is held during 20 min. The mass spectrometer was operated at 20,000 u.s^{−1},
188 with a scan range from 45 to 600 u, using electron ionization at 70 eV. Data
189 processing of the Py-GCxGC/MS raw data was achieved using a GC Image software,
190 version 2.4 (Lincoln, NE). As noted above, lacquer components were identified by
191 comparison of their mass spectra with mass spectra of the NIST library (NIST, 2011)
192 and by interpretation of the main fragmentations.

193

194 **3. Results**

195 **3.1. Microscopic observation**

196 Two lacquer film layers, ticked as the first lacquer layer and the second lacquer layer
197 on the ground layer, can be clearly observed (Fig.4A). The first layer is on the top of
198 the ground layer and the second layer is on the top of the first layer. The micrographs
199 of the lacquer base, the first lacquer layer and the second lacquer layer are separately
200 shown in Fig.4B, Fig.4C and Fig.4D, respectively. There are some white, yellow and
201 red particles, as well as some cracks visible on the ground layer in Fig.4B. Similarly,
202 there are some small white and red particles visible on the first lacquer film layer in
203 Fig.4C. Moreover, big particles on the cracks were observed on the second lacquer
204 layer in Fig.4D.

205 On observation of the whole sample cross-section, the layout of the lacquer sample
206 can be divided into three parts, a lacquer coating divisible in two parts (with a total
207 thickness of ca. 45 μm), a ground layer which is about 360-380 μm thick, and the
208 wood support as shown in Fig.4E. Depending on the angle of view, the layout of the
209 lacquer film layers can be difficult to observe as revealed on the cross-section
210 micrograph in Fig.4F. Large (300 μm*170 μm) and small (20 μm * 50 μm) white or
211 white-yellow particles can be found on the ground layer (Fig.4G and Fig.4H) .
212 Additionally, some holes can also be observed in the ground layer (Fig.4H).

213

Figure 4

214 The SEM-EDS results from the analysis of the different layers showed in Fig.5 are
215 depicted in Table 1. The main elements contained in the lacquer sample are carbon
216 (C), oxygen (O), iron (Fe), copper (Cu), lead (Pb), calcium (Ca), phosphorous (P),
217 magnesium (Mg), aluminium (Al) and silicon (Si). The content of calcium and
218 phosphorus in the ground layer is obviously higher than those observed in the lacquer
219 film layers. As reported in Fig.5B-C, distribution patterns for calcium and phosphorus
220 present a similar appearance. Combined with the Raman spectroscopy analysis results
221 (see below in section 3.2), the areas of calcium and phosphorus distribution are nicely
222 correlated to the presence of hydroxyapatite. The copper and lead distributed on the
223 cross-section may likely come from the bronze sword, whereas the silicon present
224 may likely come from the soil.

225

Figure 5

226 3.2. Raman spectroscopy analysis

227 Lacquer sample cross-section was investigated by Raman spectroscopy. The
228 corresponding Raman spectra of the large white or yellow-white particles in the
229 sample and Raman spectra of the hydroxylapatite reference ore ($\text{Ca}_{5.00}(\text{P}_{1.00}$
230 $\text{O}_4)_3((\text{OH})_{0.98}\text{Cl}_{0.02})$) ('Hydroxylapatite R060180') were shown in Fig.6. The observed
231 Raman peaks at 431, 579, 591, 609, 962, 1047, 1069 and 3574 cm^{-1} are ascribed to the
232 Raman peaks of hydroxyapatite (Timchenko et al, 2018). Small hydroxyapatite
233 particles are observed in the lacquer samples. The small particles are less than $10\text{ }\mu\text{m}$
234 in size while the larger particles are more than $300\text{ }\mu\text{m}$ in size. This may agree with
235 the use of different particle size of bone powders in different steps of lacquering craft
236 in ground layer formation (e.g., first applying large size particles to fill large holes in
237 the wooden base and then applying small size particles to smooth the surface), a
238 phenomenon previously observed in adjoining *Chu* state lacquerware (Jin et al. 2017;
239 Jin et al. 2012). Cuprite (Cu_2O), anatase (TiO_2) and carbon (amorphous) are also
240 detected on the cross-section in which the origin of cuprite was attributed to the
241 bronze sword while the origin of anatase was attributed to the soil present in the
242 buried environment (Fig.S1, supplementary material).

243

Figure 6

244 The detection of the white particles of indeterminate forms is in accordance with the
245 use of powdered bone as a ground layer demonstrated by the cross-sectional views of
246 the lacquer coating in the archaeological sample. The detection of Ca during the
247 SEM-EDX analysis (Fig.5B) confirms this statement. Detection of hydroxyapatite by

248 Raman spectroscopy also acts in favor of a presence of added crushed bones particles,
249 which is unexpected at first glance and reveals a piece of interesting information on
250 the basic technique of the *Ba* group for the preparation of elemental consolidation
251 layer.

252 3.3 Py-GC/MS analysis of lacquer origin

253 The extracted ion chromatograms (EICs) at m/z 91, 107, 108, 123, 124 are reported
254 beside the total ion chromatogram (TIC) in Fig.S2, supplementary material. Table 2
255 resumes the assignments of the detected pyrolysis products. The fragment ion at m/z
256 91, chosen for the characterization of alkylbenzenes, showed a distribution of
257 homologues with a predominant alkyl chain of C1 to C9. The characteristic fragment
258 ions at m/z 107-108 for phenol species, yielded a larger distribution spanning from C5
259 to C10 in the low homologue region, and peaks attributed to the pentadecenyl and
260 pentadecyl phenols C15 for elution times between 21-23 min (Fig.S2, supplementary
261 material). The m/z 107 fragment corresponds to a direct α C-C bond cleavage on the
262 substituted alkyl chain, and the m/z 108 fragment is issued from a retro-ene
263 rearrangement implying a hydrogen atom on the alkyl chain (Bouchoux et al., 2012).
264 Interestingly, one can notice that the ortho isomers (m/z 107) generally dominate the
265 meta isomers (m/z 108) in the distribution of alkylphenols observed in the
266 corresponding EICs. The meta isomers (m/z 108) were barely observed while the
267 complete series of ortho isomers C5-C12 and the 2-pentadecylphenol markers,
268 $C_{21}H_{36}O$ were observed in the sample analyzed under direct Py-GC/MS conditions
269 (Fig.S2, supplementary material). In comparison, catechol compounds (m/z 123, 124)
270 were barely extracted from the background signal in the chromatograms.

271 Analysis of the lacquer sample was also conducted under THM pyrolysis conditions.
272 Globally, THM-Py-GC/MS experiments gave concordant results to those reported by
273 Py-GC/MS. In accordance to Py-GC/MS results, the two characteristic catechol
274 markers 1,2-dimethoxy-pentadecylbenzene ($C_{23}H_{40}O_2$, $t_r=22.57$ min) and
275 1,2-dimethoxy-pentadecenylbenzene ($C_{23}H_{38}O_2$, $t_r=22.45$ min) were both detected in
276 the tested sample confirming the *Shengqi* origin. Noteworthy, under THM pyrolysis
277 conditions, kumanotanic acid, mazzeic acid and miyakoshic acid were detected at a low
278 ratio and their presence could be correlated to an ageing process of the urushi sample in
279 particular in presence of siccative oil as reported previously (Schilling et al. 2016;
280 Webb, Schilling, Chang 2016, Tamburini et al. 2016). In comparison to direct
281 Py-GC/MS analysis, the observed alkylbenzene series in the lacquer sample is
282 reduced: only the n-hexylbenzene was present while n-heptylbenzene and
283 n-octylbenzene were only detected at traces level. The distribution of catechols, as
284 reported in the EICs at m/z 151 and 152 (Fig.7), showed a large distribution with

285 additional catechol markers of lower side-chain length (C4-C5). The distribution of
286 fragment ions at m/z 151 and 152 was observed to extend to the pentadecenyl and
287 pentadecyl catechol C15 homologues for elution times of between 22 and 23 min, as
288 expected for a *Toxicodendron vernicifluum* sap origin (Fig.7, Table 3).

289 **Figure 7**

290 THM-Py-GC/MS permitted to refine the analytical information gained on the sample,
291 noticeably with the characterization of several fatty acid methyl esters. TIC and EICs
292 at m/z 74, characteristic fragment ions for the fatty acid methyl esters, at m/z 151 and
293 152, characteristic fragment ions for the methylated catechols are reported in Fig.7.
294 Table 3 reports the assignments of these marker ions. In fact, distribution of fatty acid
295 methyl esters was observed with a noticeable high ratio for the peaks associated to
296 palmitic and stearic methyl esters (Fig.7). As well the repartition of the lower
297 components of fatty acid methyl esters (C6-C10) showed a maximum for the C8
298 homologue (Table 3, $t_r=9.71$ min). The nonanedioic acid, dimethyl ester, also reported
299 as the dimethyl ester of the azelaic acid ($C_{11}H_{20}O_4$ $t_r = 14.57$ min), was detected in
300 association with the octanedioic acid, dimethyl ester ($C_{10}H_{18}O_4$ $t_r = 13.59$ min) and
301 the decanedioic acid, dimethyl ester ($C_{12}H_{22}O_4$ $t_r = 15.60$ min) (Fig.7, Table 3). The
302 relative proportion of azelaic acid and di-acids of longer chain as well as the presence
303 of palmitic acid were in accordance with the previous detection of those compounds
304 in aged mixtures of urushiol lacquer and drying oil (Tamburini et al., 2016).

305 **3.4 Py-GCxGC/MS analysis of the lacquer sample**

306 Due to the intrinsic grouping features of GCxGC separation (Han et al., 2018),
307 different series of compounds can be easily separated on the resulting Py-GCxGC/MS
308 chromatogram (Fig.8). Among the structures observed, the patterns of typical lacquer
309 component can be observed in the 2D chromatogram with a higher sensitivity and
310 dynamics compared to direct Py-GC/MS: (i) a series of alkane ranging from C10 to
311 C29; (ii) a series of alkene ranging from C10 to C18; (iii) a series of alkylbenzene
312 homologues ranging from C1 to C15; (iv) a series of catechols ranging from C1 to
313 C15. These four series in the Py-GCxGC/MS TIC chromatogram confirmed distinctly
314 the presence of a lacquer originating from *Toxicodendron vernicifluum*. Moreover, as
315 can be seen in the 2D chromatogram, other compounds could be patently highlighted:
316 (i) a series of PAH compounds, which cannot be obtained during classical 1D analysis,
317 (ii) a series of 2-ketones and 7-ketones, similarly difficult to detect by Py-GC/MS,
318 and (iii) other organics (methylphenones, cycloalkenes, furanones) not characterized
319 otherwise.

320

Figure 8

321 As stated above, EICs of the m/z 107-108 (characteristic fragments for the
322 alkylphenols) confirmed the *shengqi* origin of the sample in particular with the
323 detection of the characteristic C15 ortho/meta homologues. All the homologues
324 already detected during direct Py-GC/MS were detected here but with an improved
325 characterization of the lower homologues C1-C5, which were hardly extracted from
326 the TIC background during 1D analysis. Moreover, the GCxGC separation conducted
327 to a better detailed picture of positional isomer distribution of alkylphenol markers
328 with the clear differentiation of ortho and meta isomers still observable in a
329 deteriorated archaeological sample, thanks to the sensitivity of the GCxGC separation
330 (Fig.S3, Supplementary materials). Showing a decreasing intensity, the C8-C14
331 homologues provided the meta isomers for all this group while the ortho isomers were
332 slowly disappearing in the series for homologues above C9. Compare to Py-GC/MS
333 analysis, the complete series of alkylphenols from C1-C15 can be followed in the EIC
334 of m/z 107-108 ion markers of the alkylphenols. Similarly, the EICs for m/z 91 and
335 92 yielded the complete series of alkylbenzene from the C1 to C15 homologues.
336 Comparatively, as shown above, Py-GC/MS provided an alkylbenzene series from C1
337 to C11 and no detection of the characteristic C15 homologue. In addition, the lower
338 homologues of the alkylbenzene series are observable with their different positional
339 isomers. Noticeably, the C13 and C14 homologues were visible here and detected at
340 trace level.

341 EICs for the m/z 55-57 provided a longer distribution of the series of alkanes/alkenes
342 than previously observed during Py-GC/MS analysis since this series was limited to
343 the C15 homologue in 1D analysis. Here, the series of alkanes span from C10 to C29,
344 and alkenes from C10 to C18. Interestingly, if the previous pattern observed during
345 Py-GC/MS analysis with major peaks at C14, C15 are conserved, Py-GCxGC/MS
346 yielded an increased distribution of these major homologues until the C17 homologue
347 for both alkanes and alkenes. Previous results obtained with reference lacquer films
348 provided a similar pattern with the presence of alkanes and alkenes for the C14-C17
349 homologues in the case of the *Toxicodendron vernicifluum* lacquer sap differentiating
350 it from other lacquer saps (Okamoto et al., 2018). Noticeably, a series of compounds
351 was observed in the previous EIC m/z 91 for which their appearance was improved by
352 the extraction of the base peak at m/z 119 in the chromatogram. Dispersedly
353 distributed around 21-22 min (dimension 1) and ca. 5s (dimension 2), and mixed to
354 the alkylphenol homologues distribution, these compounds were assigned to
355 substituted methylphenyl, ethanone.

356 Another series of ketone compounds associated to linear structures were observed
357 between 5-62 min (dimension 1) and 3-4s (dimension 2). This series started with the
358 lower homologue: 2-hexanone (C₆H₁₂O MW 100) 5.7 min 2.96 s and continued by
359 incrementation in the number of carbons until the C18 homologue, 2-octadecanone.
360 Besides, a series of alkyl ketones assigned to alkyl, 7-one was observed from
361 C11-C17. From C10 to C12, unsaturated ketones were observed near their associated
362 2-ketones. Indeed, their detection could not be easily conducted from Py-GC/MS
363 chromatogram as these compounds are noticeably diluted in the global TIC. The fact
364 is that, after observation of this long-chain ketone series in 2D experiments, a
365 backward EIC procedure at m/z 58 for the 1D experiment could only provide a
366 limited part of these series of ketones present in the archaeological lacquer sample,
367 and definitely not their complete distribution revealed in the Py-GCxGC/MS analysis.
368 The observed series of ketones (n-alkan-2-ones) may result from the oxidative
369 burning of vegetation wax alkanes (Simoneit, 2002) as well as from the incomplete
370 combustion of aliphatic compounds (Oros and Simoneit, 2001a). Similarly,
371 α,ω -alkanedioic acids may result from the oxidation of biopolymers, of other lipid
372 compounds (e.g. ω -hydroxyalkanoic acids), or from the incomplete combustion of
373 other products. In particular, the presence of α,ω -nonanedioic acid was previously
374 rationalized through the potential photooxidation of C18:1 and C18:2 alkenoic acids
375 (Oros and Simoneit, 2001b). Nevertheless, no any trace of unsaturated fatty acids was
376 detected during our investigations.

377 PAH compounds such as naphthalene, fluorene, anthracene, phenanthrene, and pyrene
378 can be well separated and detected together with their methylated homologues (Fig.8)
379 (Table S1 Supplementary Materials). However, no markers of presence for PAH
380 derived compounds were characterized during the above direct Py-GC/MS analysis
381 (Table 2 and 3). The lack of detection of PAHs during 1D analysis can be rationalized
382 by the complexity of the components resulting in a mixture hardly resolved by a one
383 dimension GC/MS analysis. As a consequence, the detection and characterization of
384 PAHs that can hardly be fully characterized by 1D analysis constitutes one of the
385 most interesting improvement provided here by the use of the GCxGC separation.

386

387 **4. Discussion**

388 **4.1 Bone-derived ground layer of *Ba* lacquering**

389 Bone-derived ground layer (骨粉打底) has a long tradition in ancient Chinese
390 lacquering. Scholars have speculated that this tradition was early used in Han dynasty

391 (202BC-220AD) which was testified by scientific analysis of Han lacquerwares (Jin,
392 2008). Later, the discovery of bone-derived ground layer from lacquerware in
393 Jiuliandun tomb (*Chu* state) traced this tradition back to the Warring States (Jin et al.,
394 2017). The discovery of bone-derived ground layer on *Ba* state testified the previous
395 observation of Dr. Jin in lacquer wares from the Warring States period (Jin et al.,
396 2012; Jin et al., 2017). The analytical evidence supports that different size particles of
397 hydroxyapatite from bone was added to the lacquer base during its making process,
398 confirming the old recorded recipes of lacquer coating making in ancient China (Jin et
399 al., 2017) and the earliest one of *Ba* state.

400 These particles of hydroxyapatite appeared to be added to the ground layer without
401 presenting a regular and reproducible size pattern in the process of lacquer making:
402 this observation agrees with the use of different particle size of bone powders in
403 different steps of lacquering craft in ground layer formation, a phenomenon
404 previously observed in adjoining *Chu* state lacquerware (Jin et al., 2017; Jin et al.,
405 2012). Due to the cracks, the application steps of different size bone particles cannot
406 be clearly differentiated in the tested samples. The same traditions found in *Ba* state
407 and *Chu* state showed evident similarity in the lacquering, inferring the cultural and
408 craft communications between these two adjoining states. In addition, ground layer
409 with other composition or no ground layer (Wei et al., 2011; Fu et al., 2020) has also
410 been reported which showed diversified lacquer crafting during the Warring States.
411 Down from this period, this tradition has a long and wide use that can be often found
412 in old Korean lacquerware and Chinese old lacquerware while the Japanese
413 lacquerware doesn't show such powdered bone foundation (Urushi 1988; Hao et al,
414 2021).

415 **4.2 Lacquer sap and drying oil in *Ba* lacquerware**

416 If the use of drying oil like tung oil has been previously characterized in Japanese
417 export lacquer from modern time (Heginbotham and Schilling, 2011), the use of tung
418 oil has been mostly documented in Chinese lacquer (Hao et al., 2019; Tamburini et al.,
419 2015) and the concomitant detection of oil and lacquer mixture in archaeological
420 samples is always a matter of interest to increase our knowledge on lacquer
421 fabrication. In previous experiments associating urushi lacquer and tung oil as a
422 mixture, a relatively low abundance of azelaic acid was reported and its low
423 abundance was correlated to the presence of induced cross-linking at a higher degree
424 when the oil was added to urushi (Tamburini et al. 2016). Additionally, during the
425 same experiments, the proportion of short chain fatty acids was observed to increase.
426 Noticeably, under the THM pyrolysis conditions applied here, numerous fatty acids

427 C6-C10 were observed (Table 3), an observation in accordance with the addition of
428 drying oil in the sample. In the absence of any other contradiction, assumption of the
429 use of tung oil can be considered in view of its previous detection in Asian lacquer
430 (Hao et al., 2019; Tamburini et al. 2015).

431 The presence of drying oil was observed previously in ancient samples dated from the
432 Jōmon period in Japan, suggesting that the mastered technic of mixing lacquer sap
433 with dry oil in the purpose of increasing luster and elastic of lacquer film was early
434 employed in the premise of lacquer making technique (Yuasa et al., 2015). Drying
435 oils have also been characterized recently in Chinese lacquer samples of the Warring
436 States period (Fu et al., 2020) and even, feasibility studies have been attempted to
437 quantify drying oil in ancient lacquerwares using FTIR spectroscopy (Xiao et al.,
438 2020). The detection of markers of potential drying oil addition in the sample of the
439 *Ba* ethnic group is in accordance with these experiments. The formation of azelaic
440 acid, as well as the formation of other similar dicarboxylic acids rationalized by
441 oxidation processes of polyunsaturated fatty acids, can be proposed as a manifestation
442 of an autoxidation phenomenon of drying oils present in the sample (Tamburini et al.,
443 2016). However, the possibility that formation of these dicarboxylic acids results from
444 the oxidation of soot components cannot be completely ruled out, at the present state
445 of investigations, and must be kept as an assumption (Oros and Simmoneit, 2001a,
446 2001b).

447 **4.3 Soot additives revealed by GCxGC separation**

448 As reported in the table of assignment of PAH related homologues (Table S1,
449 Supplementary materials), we observed more easily the presence of
450 methylphenanthrenes and dimethylphenanthrenes than the same homologues for
451 anthracene, methyl- and dimethylanthracenes in the lacquer sample. A lower
452 abundance of alkylanthracenes compared to alkylphenanthrenes in sedimentary rocks
453 is proposed to account for a widespread terpenoid origin to explain the presence of
454 alkylphenanthrenes (Smith et al., 1995): this fact correlates well with the use of plant
455 soot as black carbon source in the elemental consolidation lacquer layer of the
456 wooden scabbard. Indeed, the absence of structures commonly related to pyrolytic
457 PAHs like benzo[e]pyrene, benzo[a]pyrene, benzofluoranthenes, is in accordance
458 with the soot origin of the detected PAH homologues acting as a coloring material in
459 the fabrication of lacquer artifacts belonging to the Warring States period.

460 However, assignment of the origin of PAHs in archaeological remains a matter of
461 discussion and shows difficulties in defining attribution of originating processes (Zou
462 et al., 2010). The absence of terpenic markers could act in the use of other species

463 than softwood species (e.g., pines, spruces, larches). In particular, retene, a
464 well-known marker of abietic acid degradation was absent, which casts doubt on the
465 use of pine wood species (Ren et al., 2018; Karp et al., 2020). Conversely, if the
466 detection of an enlarged series of alkane homologues by Py-GCxGC/MS could be
467 correlated with combustion processes of pine wood species, specificity of these
468 alkanes/alkenes as wood markers is questionable (Simoneit, 2002). More
469 interestingly, the presence of the mono-, di-, tri-methylated PAHs (naphthalene,
470 anthracene, pyrene) may be correlated to the use of a wood species with bark as
471 material for soot making (Achten et al., 2015).

472

473 **5. Conclusion**

474 In this paper, composition of the lacquer layers of the scabbard of a bronze sword
475 dating from the Warring States (475-221 BC) and excavated from a *Ba* tomb of the
476 Lijiaba site (Chongqing, southwest China) was investigated. Based on the
477 experimental results obtained in the course of a multidisciplinary approach, the
478 lacquer material constitutive of the decorative coating of the wooden scabbard was
479 assigned to *Shengqi* origin with the characterization of chemical markers of
480 *Toxicodendron vernicifluum* lacquer trees. Additionally, the detection of
481 hydroxyapatite particles and the cartography of chemical elements in the sample are
482 in accordance with the use of crushed bone material in the composition of the ground
483 layer of lacquer. Worthy of mention, Py-GC/MS analysis of the scabbard lacquer
484 sample conducted to the assignment of origin for the lacquer sap and suggested the
485 presence of drying oil addition in relation to the lacquer-making recipes, whilst
486 Py-GCxGC/MS, due to its sensibility and extended resolution, demonstrated
487 unequivocally the presence of other compounds, and particularly PAHs which are
488 attributed to the use of soot of plant origin for coloring of the lacquer.

489 The present study, which investigated for the first time an archaeological sample of
490 the *Ba* ethnic group of southwest China, permitted to increase our knowledge of the
491 lacquer making crafts of *Ba* state that has been hindered until now due to the rareness
492 of lacquer samples unearthed in ancient *Ba* state locations. Moreover, the present
493 experimental study provides the base for the comparison of lacquer samples coming
494 from adjacent regions and central states upon further study of valuable interest to
495 introduce connection between craft shift, manufacturing techniques and chemical
496 analysis strategies. In light of the present work, future research combining the
497 techniques employed here should permit further investigations of the ancient lacquer

498 craft in China to refine data and to explore existing relationships between ethnic
499 groups in the sharing of lacquer manufacturing techniques.

500

501 **Funding:** BH thanks to the Fundamental Research Funds for the Central Universities
502 and Postdoctoral Science Foundation for support.

503

504 **Declarations of interest:** none

505

506 References

- 507 Achten, C., Beer, F.T., Stader, C., Brinkhaus, S.G., 2015. Wood-specific polycyclic
508 aromatic hydrocarbon (PAH) patterns in soot using gas
509 chromatography-atmospheric pressure laser ionization-mass spectrometry
510 (GC-APLI-MS). *Environ. Forensics* 16, 42-50.
511 <https://doi-org.proxy.mnhn.fr/10.1080/15275922.2014.991004>.
- 512 Heginbotham, A., Chang, J., Khanjian, H., Schilling, M.R., 2016. "Some
513 Observations on the Composition of Chinese Lacquer." *Studies in*
514 *Conservation* 61 (sup3): 28-37.
515 <https://doi.org/10.1080/00393630.2016.1230979>.
- 516 Avataneo, C., Sablier, M., 2017. New criteria for the characterization of traditional
517 East Asian papers. *Environ. Sci. Pollut. Res.* 24(2), 2166-2181.
518 <https://doi.org/10.1007/s11356-016-6545-0>.
- 519 Bai, J., 2020. The Ba culture in the field of archaeometry: conception, problem and
520 method. *Yangtze River Civilization*, 3, 1-11. (in Chinese).
- 521 Bouchoux, G., Sablier, M., Miyakoshi, T., Honda, T., 2012. A 'meta effect' in the
522 fragmentation reactions of ionised alkyl phenols and alkyl anisoles. *J. Mass*
523 *Spectrom.* 47, 539-46. <https://doi.org/10.1002/jms.2977>.
- 524 Challinor, J. M., 2001. Review: the development and applications of thermally
525 assisted hydrolysis and methylation reactions. *J. Anal. Appl. Pyr.* 61, 3-34.
- 526 Chongqing, 2001. *Collections of reports on the archaeological excavation in the three*
527 *Gorges Dam, Chongqing in 1997* (Sciences Press: Beijing).
- 528 Chongqing, 2003. *Collections of reports on the archaeological excavation in the three*
529 *Gorges Dam, Chongqing in 1998* (Sciences Press: Beijing).
- 530 Fan, X., Freestone I.C., 2017. Occurrence of phosphatic corrosion products on bronze
531 swords of the Warring States period buried at Lijiaba site in Chongqing,
532 China. *Heritage Sci.* 5, 48. <https://doi.org/10.1186/s40494-017-0161-2>.
- 533 Fan, X., Wang, Q., Wang, Y., 2020. Non-destructive in situ Raman spectroscopic
534 investigation of corrosion products on the bronze dagger-axes from Yujiaba
535 site in Chongqing, China. *Archaeol Anthropol Sci* 12, 90.
536 <https://doi.org/10.1007/s12520-020-01042-0>
- 537 Fu, Y., Chen, Z., Zhou, S., Wei, S., 2020. Comparative study of the materials and
538 lacquering techniques of the lacquer objects from Warring States Period
539 China. *J. Archaeological Sci.* 114, 105060.
540 <https://doi.org/10.1016/j.jas.2019.105060>.
- 541 Han, B., Lob, S., Sablier, M., 2018. Benefit of the Use of GCxGC/MS Profiles for 1D
542 GC/MS Data Treatment Illustrated by the Analysis of Pyrolysis Products from
543 East Asian Handmade Papers. *J. Am. Soc. Mass Spectrom.* 29, 1582–1593.
544 <https://doi.org/10.1007/s13361-018-1953-7>
- 545 Hao, X., Wu, H., Zhao, Y. et al, 2017. Analysis on the Composition/structure and
546 Lacquering Techniques of the Coffin of Emperor Qianlong Excavated from

547 the Eastern Imperial Tombs. *Sci. Rep.* 7, 8446 1-11.
548 <https://doi.org/10.1038/s41598-017-08933-8>

549 Hao, X., Schilling, M. R., Wang, X., Khanjian, H., Heginbotham, A., Han, J., Auffret,
550 S., Wu, X., Fang, B., Tong, H. 2019. "Use of THM-PY-GC/MS Technique to
551 Characterize Complex, Multilayered Chinese Lacquer." *Journal of Analytical
552 and Applied Pyrolysis* 140 (June): 339-48.
553 <https://doi.org/10.1016/j.jaap.2019.04.011>.

554 Hao, X., Wang, X., Zhao, Y., Tong, T., Gong, Y., 2021. Identification of minerals and
555 mineral pigments in lacquer by the comprehensive comparative analysis of
556 spectroscopy information, *Spectroscopy Letters*, 54:6, 446-457, DOI:
557 10.1080/00387010.2021.1940208

558 Heginbotham, A., Schilling, M., 2011. New Evidence for the use of Southeast Asian
559 raw materials in seventeenth-century Japanese export lacquer, in: S. Rivers, R.
560 Faulkner, R. Boris Pretzel (Eds.), *East Asian Lacquer: Material Culture,
561 Science and Conservation*, Archetype Publications, London, pp. 92-106.

562 Heginbotham, A., Chang, J., Herant, K., Schilling, M.R., 2016. "Some Observations
563 on the Composition of Chinese Lacquer." *Studies in Conservation* 61 (sup3):
564 28-37. <https://doi.org/10.1080/00393630.2016.1230979>.

565 'Hydroxylapatite R060180'. <http://rruff.info/apatite/display=default/R060180>.

566 Jin, P.J., 2008. *The Lacquering Technique of Han Dynasty*. University of Science and
567 Technology of China.

568 Jin, P.J., Hu, Y.L., Ke, Z.B., 2017. Characterization of lacquer films from the middle
569 and late Chinese warring states period 476–221BC. *Microscopy Res. Techn.*
570 80, 1344-50. <https://doi.org/10.1002/jemt.22947>.

571 Jin P.J., Hu Y., Gu X., Ji X., 2012. Research on the Making Techniques about
572 Lacquer Plaster Layer of Lacquer Wares Excavated from Jiuliandun Tombs
573 [J]. *Jiangnan Archaeology*. (in Chinese)

574 Karp, A.T., Holman, A.I., Hopper, P., Grice, K., Freeman, K.H., 2020. Fire
575 distinguishers: Refined interpretations of polycyclic aromatic hydrocarbons
576 for paleo-applications. *Geochimica Cosmochimica Acta* 289, 93–113.
577 <https://doi.org/10.1016/j.gca.2020.08.024>.

578 Karpova, E., Nefedov, A., Mamatyuk, V., Polosmak, N., Kundo, L., 2017.
579 Multi-analytical approach (SEM-EDS, FTIR, Py-GC/MS) to characterize the
580 lacquer objects from Xiongnu burial complex (Noin-Ula, Mongolia).
581 *Microchemical J.* 130, 336-44. <https://doi.org/10.1016/j.microc.2016.10.013>.

582 Le Hô, A.-S., Regert, M., Marescot, O., Duhamel, C., Langlois, J., Miyakoshi, T.,
583 Genty, C., Sablier, M., 2012. Molecular criteria for discriminating museum
584 Asian lacquerware from different vegetal origins by pyrolysis gas
585 chromatography/mass spectrometry. *Anal. Chim. Acta* 710, 9-16.
586 <https://doi.org/10.1016/j.aca.2011.10.024>.

587 Lu, R., Honda, T., Miyakoshi, T., 2012. 'Application of Pyrolysis-Gas
588 Chromatography/Mass Spectrometry to the Analysis of Lacquer Film.' in Dr.
589 Mustafa Ali Mohd (ed.), *Advanced Gas Chromatography-Progress in*

590 *Agricultural, Biomedical and Industrial Applications* (InTech Europe 2012,
591 Croatia.).

592 Ma, X., Lu, R., Miyakoshi, T., 2014. Application of Pyrolysis Gas
593 Chromatography/Mass Spectrometry in Lacquer Research: A Review.
594 *Polymers* 6, 132-44. <https://doi.org/10.3390/polym6010132>.

595 NIST Mass Spec Data Center, S.E. Stein, director (2011) “Mass Spectra” in
596 WebBook of Chemistry, NIST Standard Reference Database Number 69, Eds.
597 P.J. Linstrom and W.G. Mallard, National Institute of Standards and
598 Technology, Gaithersburg MD, 20899, <http://webbook.nist.gov>

599 Okamoto, S., Honda, T., Miyakoshi, T., Han, B., Sablier, M., 2018. Application of
600 pyrolysis-comprehensive gas chromatography/mass spectrometry for
601 identification of Asian lacquers. *Talanta* 189, 315-23.
602 <https://doi.org/10.1016/j.talanta.2018.06.079>.

603 Oros, D.R., Simoneit B.R.T., 2001a. Identification and emission factors of molecular
604 tracers in organic aerosols from biomass burning Part 1. Temperate climate
605 conifers. *Appl. Geochem.* 16, 1513-1544.
606 [https://doi.org/10.1016/S0883-2927\(01\)00021-X](https://doi.org/10.1016/S0883-2927(01)00021-X).

607 Oros, D.R., Simoneit B.R.T., 2001b. Identification and emission factors of molecular
608 tracers in organic aerosols from biomass burning Part 2. Deciduous trees.
609 *Appl. Geochem.* 16, 1545-1565.
610 [https://doi.org/10.1016/S0883-2927\(01\)00022-1](https://doi.org/10.1016/S0883-2927(01)00022-1).

611 Ren, M., Wang, R., Yang, Y. 2018. Identification of the proto-inkstone by organic
612 residue analysis: a case study from the Changle Cemetery in China. *Herit Sci*
613 6, 19. <https://doi.org/10.1186/s40494-018-0184-3>

614 Schilling, M.R., Heginbotham, A., van Keulen, H., Szelewski, M., 2016. Beyond the
615 basics: A systematic approach for comprehensive analysis of organic materials
616 in Asian lacquers. *Studies in Conservation* 61, 3-27.
617 <https://doi.org/10.1080/00393630.2016.1230978>.

618 Simoneit B. R.T., 2002. Biomass burning — a review of organic tracers for smoke
619 from incomplete combustion. *Applied Geochem.* 17, 129–162.
620 [https://doi.org/10.1016/S0883-2927\(01\)00061-0](https://doi.org/10.1016/S0883-2927(01)00061-0).

621 Smith, J. W., George, S. C., Batts, B. D., 1995. The geosynthesis of alkylaromatics.
622 *Org. Geochem.* 23(1), 71-80. [https://doi.org/10.1016/0146-6380\(94\)00101-6](https://doi.org/10.1016/0146-6380(94)00101-6).

623 Tamburini, D., Bonaduce, I., Colombini, M.P., 2015. Characterization and
624 identification of urushi using in situ Pyrolysis/silylation-Gas
625 Chromatography-Mass Spectrometry. *J. Anal. Applied Pyr.* 111:33-40
626 <https://doi.org/10.1016/j.jaap.2014.12.018>.

627 Tamburini, D., Sardi, D., Spepi, A., Duce, C., Tinè, M.R., Colombini, M.P.,
628 Bonaduce, I., 2016. An investigation into the curing of urushi and tung oil
629 films by thermoanalytical and mass spectrometric techniques. *Polymer*
630 *Degrad. Stability* 134, 251-64.
631 <https://doi.org/10.1016/j.polymdegradstab.2016.10.015>.

632 Timchenko, P. E., Timchenko, E. V., Pisareva, E. V., Vlasov, M. Y., Volova, L. T.,
633 Frolov, O. O., Kalimullina, A. R., 2018. Experimental studies of

634 hydroxyapatite by Raman spectroscopy. *Journal of optical technology*, 85(3),
635 130-135.

636 Urushi: Proceedings of the 1985 Urushi Study Group, N.S. Brommelle and Perry
637 Smith, editors. 1988 J. Paul Getty Trust.

638 Wan, Y-Y, Lu R., Du Y-M., Honda T., Miyakoshi T.. 2007. "Does Donglan Lacquer
639 Tree Belong to *Rhus Vernicifera* Species?" *International Journal of Biological*
640 *Macromolecules* 41 (5): 497-503.

641 Webb, M., Schilling, M.R., Chang, J., 2016. The reproduction of realistic samples of
642 Chinese export lacquer for research. *Studies in Conservation* 61, 155-65.
643 <https://doi.org/10.1080/00393630.2016.1227116>.

644 Wei, S., Pintus, V., Pitthard, V., Schreiner, M., Song, G., 2011. Analytical
645 characterization of lacquer objects excavated from a Chu tomb in China. *J.*
646 *Archaeological Sci.* 38, 2667-74. <https://doi.org/10.1016/j.jas.2011.05.026>.

647 Wu, Q.Q., Zhu, J.J., Liu, M.T., Zhou, Z., An, Z., Huang, W., He, Y.H., Zhao, D.Y.,
648 2013. PIXE-RBS analysis on potteries unearthed from Lijiaba Site. *Nuclear*
649 *Instruments and Methods in Physics Research Section B: Beam Interactions*
650 *with Materials and Atoms* 296, 1-6.
651 <https://doi.org/10.1016/j.nimb.2012.12.004>.

652 Xiao, Q., Wei, S., Fu, Y-C., 2020. Feasibility Study on Quantitative Analysis of
653 Ancient Lacquer Films by Infrared Spectroscopy. *Spectroscopy Spectral*
654 *Analysis* 40(9), 2962-2967.

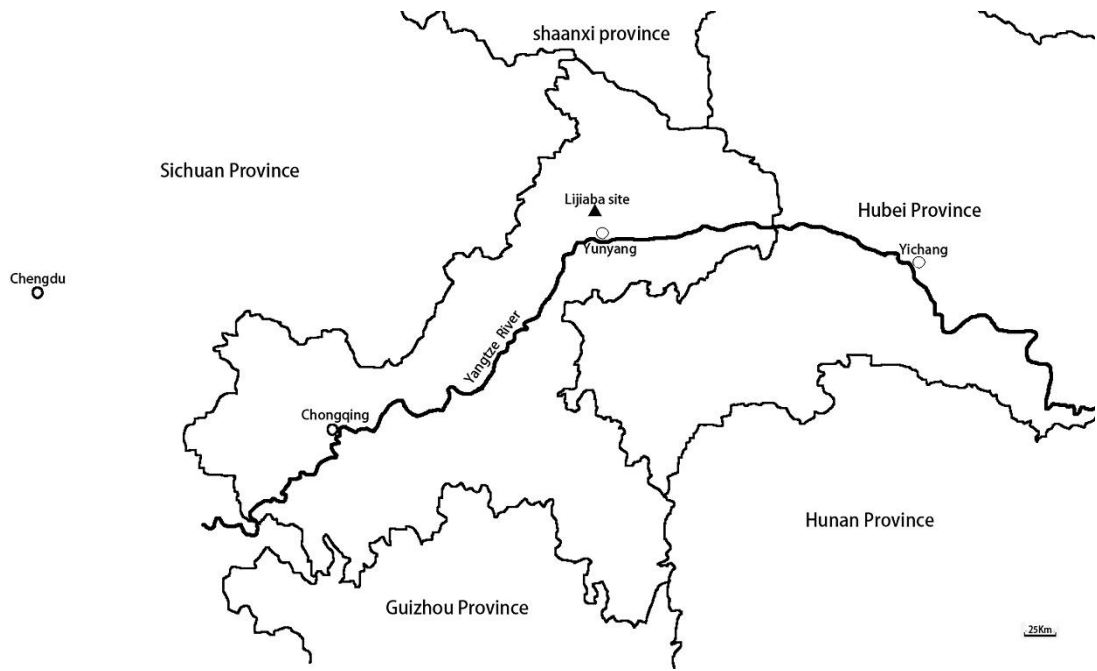
655 Yuasa, K., Honda, T., Lu, R., Hachiya, T., Miyakoshi, T., 2015. Analysis of Japanese
656 ancient lacquerwares excavated from Jomon period ruins. *J. Anal. Appl. Pyr.*
657 113: 73–77. <https://doi.org/10.1016/j.jaap.2014.10.018>.

658 Zheng, L., Wang, L., Zhao, X., Yang, J., Zhang, M., Wang, Y., 2020.
659 Characterization of the materials and techniques of a birthday inscribed
660 lacquer plaque of the Qing Dynasty. *Heritage Sci.* 8(116), 1-10.
661 <https://doi.org/10.1186/s40494-020-00462-4>.

662 Zhai, K., Sun, G., Zheng, Y., Wu, M., Zhang, B., Zhu, L., & Hu, Q. (2021). The
663 earliest lacquerwares of China were discovered at Jingtoushan site in the
664 Yangtze River Delta. *Archaeometry*, 1– 9. <https://doi.org/10.1111/arc.12698>

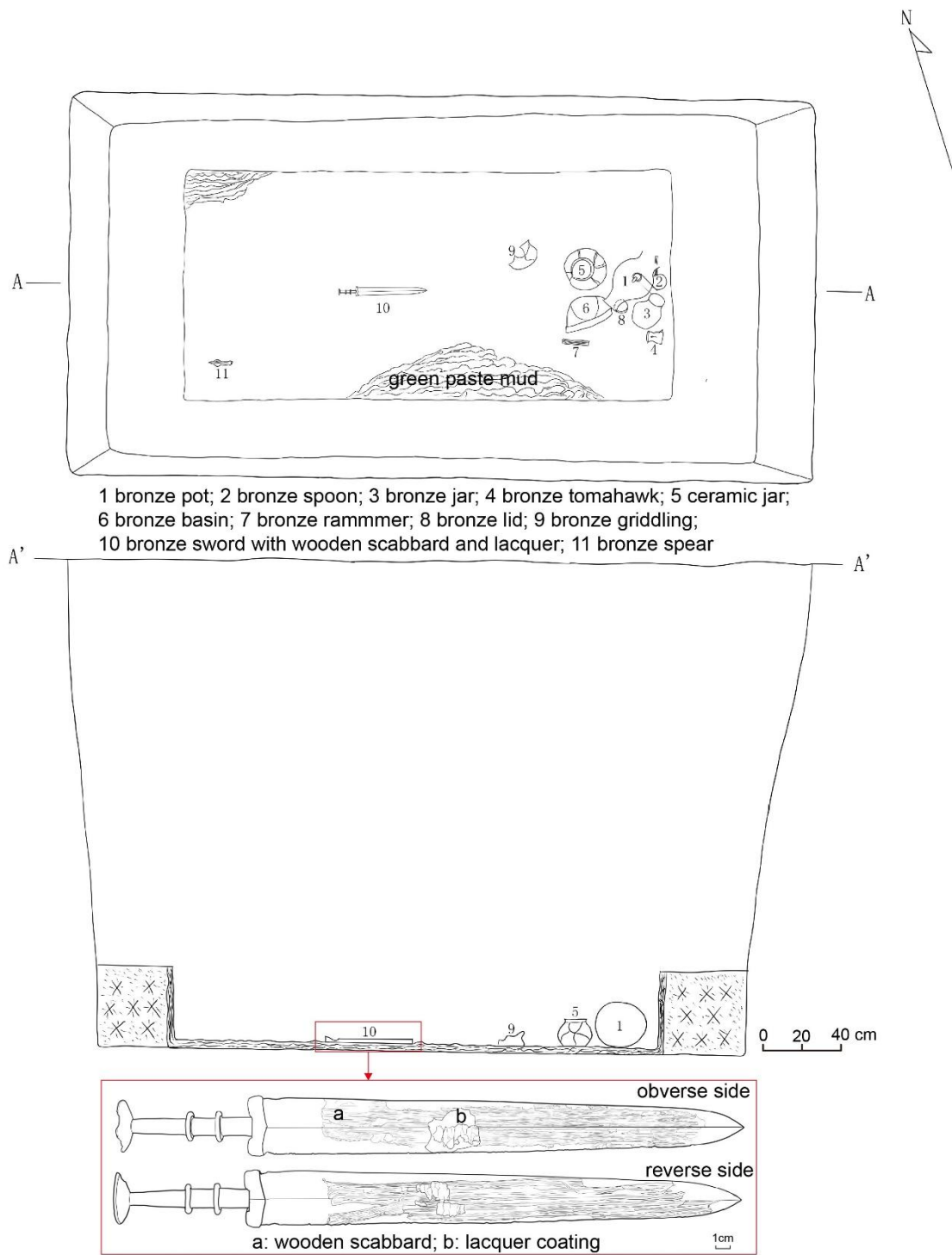
665 Zou, S., Li, R., Xie, S., Zhu, J., Wang, X., Huang, J., 2010. Paleofire indicated by
666 polycyclic aromatic hydrocarbons in soil of Jinluojia archaeological site,
667 Hubei, China. *J. Earth Sci.* 21, 247-56.
668 <https://doi.org/10.1007/s12583-010-0089-x>.

669



670

671 Fig.1. Location map of the Lijiaba site.



673

674 Fig.2. Plan of the tomb and list of the objects found.

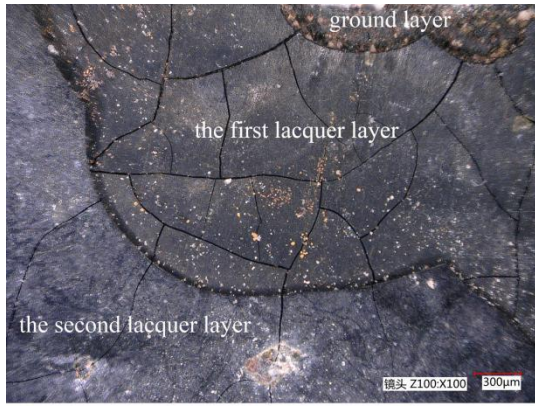
675



676

677 Fig.3. Photograph of the bronze sword with its scabbard (archaeological number
678 03YLM11:10).

679



A



B



C



D



E



F



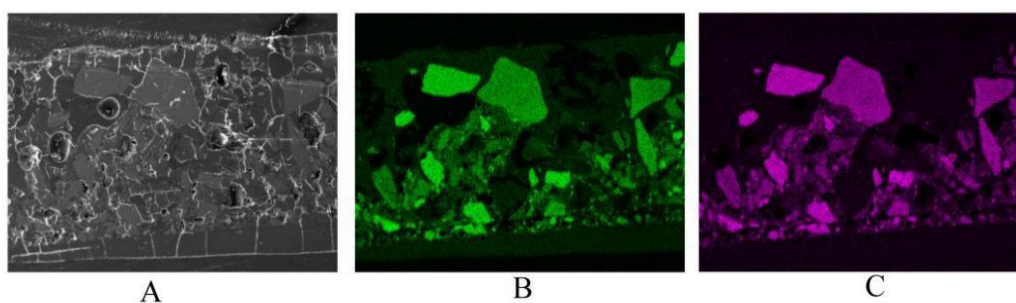
G



H

681 Fig.4. The surface micrographs of lacquer sample from Lijiaba site: (A) lacquer
682 sample (B) ground layer, (C) the first lacquer layer, (D) the second lacquer layer.
683 Cross-section micrographs of lacquer sample from Lijiaba site: (E) whole lacquer
684 sample cross-section, (F) cross-section of the lacquer film layers, (G, H) cross-section
685 of the ground layer.

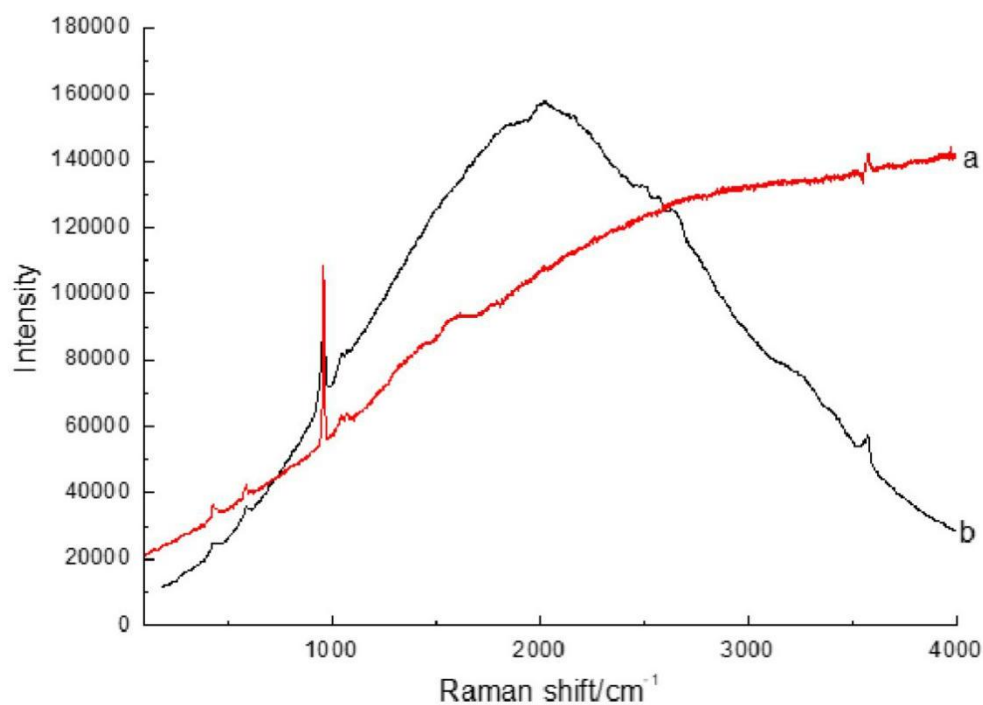
686



687

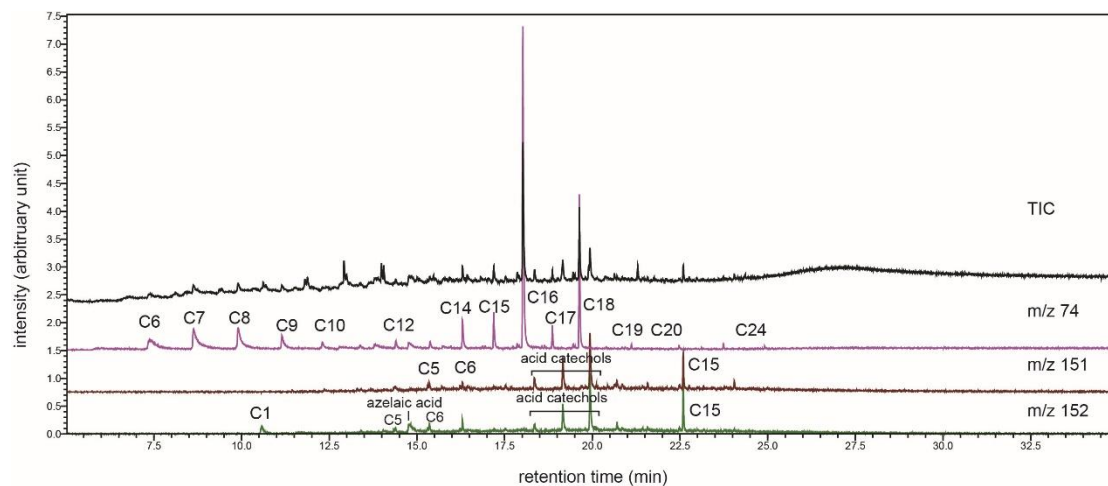
688 Fig.5. SEM-EDS elemental maps of Ca and P (A) SEM image of the analyzed area,
689 (B) SEM-EDS elemental map of Ca, (C) SEM-EDS elemental map of P.

690



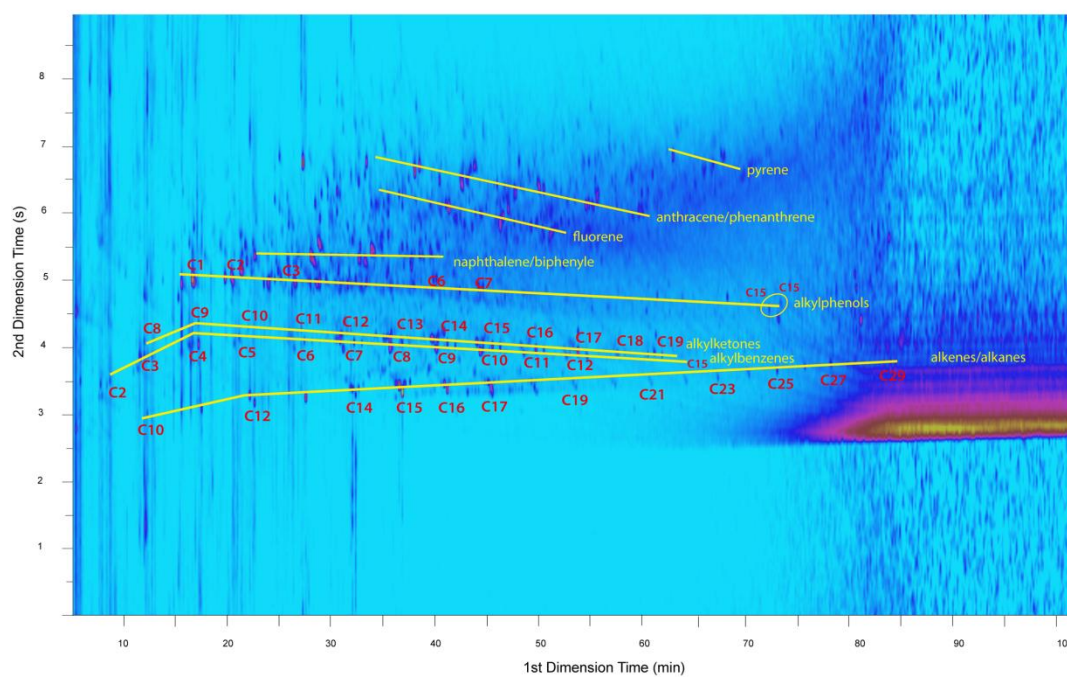
691

692 Fig.6 The Raman spectra of the lacquer samples and a standard ore (a: lacquer sample,
693 b: (Ca_{5.00} (P_{1.00} O₄)₃((OH)_{0.98} Cl_{0.02}))



694

695 Fig.7. The chromatograms obtained after pyrolysis of the tested sample under
 696 THM-Py-GC/MS where the total ion current (upper trace) and extracted ion
 697 chromatograms at m/z 74, 151, 152 are reported (see text for further description).



698

699 Fig.8. the 2D chromatogram of the lacquer sample.

700

701

Table 1. SEM-EDS results of the lacquer sample analysis

Analysis area		C	O	Fe	Cu	Pb	Ca	P	Mg	Al	Si	S	K
First lacquer film layer	1	44.52	41.11	7.37	2.76	0.05	0.01	0.03	0.28	1.8	2.00	0.03	0.03
	2	48.71	39.26	6.13	2.44	0.09	0.07	0.00	0.18	1.4	1.59	0.05	0.07
	3	58.61	31.46	5.36	3.36	0.04	0.04	0.02	0.21	0.46	0.39	0.05	0.01
Second lacquer film layer	1	46.1	40.02	5.00	3.85	0.4	0.2	0.04	0.29	1.74	2.14	0.08	0.14
	2	34.97	45.53	6.92	2.69	0.24	0.17	0.03	0.51	3.64	4.95	0.06	0.30
Ground layer	1	44.69	35.63	5.76	7.6	0.65	0.84	0.59	0.26	1.63	2.16	0.05	0.14
	2	44.5	36.48	5.62	4.46	0.36	2.05	0.77	0.32	2.14	2.78	0.09	0.43
	3	40.48	27.45	2.09	19.67	1.27	3.87	1.74	0.1	0.56	2.58	0.06	0.13

703

704 Table 2. Assignment of the main markers detected by Py-GC/MS in the investigated
705 lacquer sample with retention time (t_r), main fragment ions, expected molecular
706 weights, assigned formula and most likely attribution of the products.

Compounds	t_r (min)	fragment ions (in decreasing order of intensity)	MW	formula	assignment
Alkanes, alkenes					
	3.27	43,41,57,71,56		C ₇ H ₁₆	n-Heptane
	4.85	43,41,85,55,57	114	C ₈ H ₁₈	n-Octane
	6.46	43,57,91,41,85	128	C ₉ H ₂₀	n-Nonane
	7.99	57,43,71,41,70	142	C ₁₀ H ₂₂	n-Decane
	9.28	55,69,56,41,70	154	C ₁₁ H ₂₂	1-Undecene
	9.36	57,43,41,71,85	156	C ₁₁ H ₂₄	n-Undecane
	10.54	55,41,69,43,56	168	C ₁₂ H ₂₄	1-Dodecene
	10.64	57,43,41,71,85	170	C ₁₂ H ₂₆	n-Dodecane
	11.75	55,43,41,69,56	182	C ₁₃ H ₂₆	1-Tridecene
	11.83	57,43,71,85,41	184	C ₁₃ H ₂₈	n-Tridecane
	12.88	55,69,43,41,57	196	C ₁₄ H ₂₈	1-Tetradecene
	12.96	57,43,71,41,85	198	C ₁₄ H ₃₀	n-Tetradecane
	13.96	43,57,55,83,41	210	C ₁₅ H ₃₀	1-Pentadecene
	14.04	57,43,71,85,41	212	C ₁₅ H ₃₂	n-Pentadecane
alkylbenzenes					
	4.40	91,92,65,63,51	92	C ₇ H ₈	toluene

	6.03	91,106,65,77,51	106	C ₈ H ₁₀	Ethylbenzene
	7.50	91,120,92,65,105	120	C ₉ H ₁₂	n-Propylbenzene
	8.86	91,92,134,115,65	134	C ₁₀ H ₁₄	n-Butylbenzene
	10.23	91,92,83,55	148	C ₁₁ H ₁₆	n-Pentylbenzene
	11.48	91,92,105,43,162	162	C ₁₂ H ₁₈	n-Hexylbenzene
	12.68	92,91, 65,176	176	C ₁₃ H ₂₀	n-Heptylbenzene
	13.79	92, 91,43,79,105	190	C ₁₄ H ₂₂	n-Octylbenzene
	14.86	92,91,41,55,69	204	C ₁₅ H ₂₄	n-Nonylbenzene
alkylphenols					
	13.42	107,108,123,164,77	164	C ₁₁ H ₁₆ O	2-Pentylphenol ^t
	14.46	107,108,155,77,137	178	C ₁₂ H ₁₈ O	2-Hexylphenol
	15.44	107,108,77,79,192	192	C ₁₃ H ₂₀ O	2- Heptylphenol
	16.40	107,108,77,119,206	206	C ₁₄ H ₂₂ O	2-Octylphenol ^t
	17.31	107,108,136,220,165	220	C ₁₅ H ₂₄ O	2-Nonylphenol ^t
	22.02	107,108,304,43,94	304	C ₂₁ H ₃₆ O	2-Pentadecylphenol
Monocarboxylic fatty acid					
	18.33	73, 43,57,60,41	256	C ₁₆ H ₃₂ O ₂	Hexadecanoic acid (palmitic acid) ^t
	19.90	73, 43,57,60,55	284	C ₁₈ H ₃₆ O ₂	Octadecanoic acid (stearic acid) ^t

707 * co-elution, superscript ^t means that only a trace of compounds was detected

708

709 Table 3. Assignment of the main markers detected by THM Py-GC/MS in the
710 investigated lacquer sample with retention time (t_r), main fragment ions, expected
711 molecular weights, assigned formula and most likely attribution of the products.

Compounds	t _r (min)	fragment ions (in decreasing order of intensity)	MW	formula	assignment
Alkanes, alkenes					
	6.42	43,57,91,41,85	128	C ₉ H ₂₀	n-Nonane
	7.90	41,55,56,43,70	140	C ₁₀ H ₂₀	1-Decene
	7.99	57,43,71,41,70	142	C ₁₀ H ₂₂	n-Decane
	9.25	55,69,56,41,70	154	C ₁₁ H ₂₂	1-Undecene
	9.34	57,43,41,71,85	156	C ₁₁ H ₂₄	n-Undecane
	10.53	55,41,69,43,56	168	C ₁₂ H ₂₆	1-Dodecene
	10.62	57,43,41,71,85	170	C ₁₂ H ₂₆	n-Dodecane
	11.75	55,43,41,69,56	182	C ₁₃ H ₂₆	1-Tridecene
	11.82	57,43,71,85,41	184	C ₁₃ H ₂₈	n-Tridecane
	12.86	55,69,43,41,57	196	C ₁₄ H ₂₈	1-Tetradecene
	12.95	57,43,71,41,85	198	C ₁₄ H ₃₀	n-Tetradecane
	13.93	43,57,55,83,41	210	C ₁₅ H ₃₀	1-Pentadecene

	14.00	57,43,71,85,41	212	C ₁₅ H ₃₂	n-Pentadecane	
alkylbenzenes						
	11.45	91,92,65,79,162	162	C ₁₂ H ₁₈	n-Hexylbenzene	
	12.64	92,91, 65,176	176	C ₁₃ H ₂₀	n-Heptylbenzene †	
	13.75	92,55,91,190	190	C ₁₄ H ₂₂	n-Octylbenzene* †	
Methyl ester acid catechols						
	18.30	136,151,91,266,152	266	C ₁₅ H ₂₂ O ₄	Methyl-6-(2,3-dimethoxyphenyl)hexanoate (miyamic acid)	
	19.10	136,151,152,91,280	280	C ₁₆ H ₂₄ O ₄	Methyl-7-(2,3-dimethoxyphenyl)heptanoate (kumanotanic acid)	
	19.89	136,152,151,294,91	294	C ₁₇ H ₂₆ O ₄	Methyl-8-(2,3-dimethoxyphenyl)octanoate (mazzoic acid)	
	20.45	136,152,151,308,91	308	C ₁₈ H ₂₈ O ₄	Methyl-9-(2,3-dimethoxyphenyl)nonanoate (myakoshic acid)	
Substituted dimethoxybenzenes						
	10.46	152,109,137,79,91	152	C ₉ H ₁₂ O ₂	1,2-dimethoxy-4-methyl- (homoveratrole)	benzene
	13.22	136,91,151,141,192	192	C ₁₂ H ₁₆ O ₂	1,2-dimethoxy-3-butenylbenzene	
	13.34	136,91,152,151,194	194	C ₁₂ H ₁₈ O ₂	1,2-dimethoxy-3-butylbenzene	
	14.28	136,151,91,121,206	206	C ₁₃ H ₁₈ O ₂	1,2-dimethoxy-3-pentenylbenzene	
	14.34	208,136,151,152,	208	C ₁₃ H ₂₀ O ₂	1,2-dimethoxy-3-pentylbenzene	
	15.25	136,151,152,91,121	220	C ₁₄ H ₂₀ O ₂	1,2-dimethoxy-3-hexenylbenzene	
	15.31	136,152,137,151,91	222	C ₁₄ H ₂₂ O ₂	1,2-dimethoxy-3-hexylbenzene*	
	16.20	136,91,151,152,138	234	C ₁₅ H ₂₂ O ₂	1,2-dimethoxy-3-heptenylbenzene	
	16.26	136,236,152,151,91	236	C ₁₅ H ₂₄ O ₂	1,2-dimethoxy-3-heptylbenzene*	
	22.45	151,152,136,346,91	346	C ₂₃ H ₃₈ O ₂	1,2-dimethoxy-pentadecenylbenzene †	
	22.57	152,348,151,136,91	348	C ₂₃ H ₄₀ O ₂	1,2-dimethoxy-pentadecylbenzene	
Mono- and dicarboxylic fatty acid methyl esters						
	6.96	74,43,59,41,87	130	C ₇ H ₁₄ O ₂	Hexanoic acid, methyl ester	
	8.40	74,43,41,87,55	144	C ₈ H ₁₆ O ₂	Heptanoic acid, methyl ester	
	9.64	74,55,96,82,41	156	C ₉ H ₁₆ O ₂	4-Octenoic acid, methyl ester	
	9.71	74,87,43,41,55	158	C ₉ H ₁₈ O ₂	Octanoic acid, methyl ester	
	10.99	74,87,43,41,55	172	C ₁₀ H ₂₀ O ₂	Nonanoic acid, methyl ester	
	12.18	74,87,43,41,55	186	C ₁₁ H ₂₂ O ₂	Decanoic acid, methyl ester	
	13.59	69,55,74,67,97	202	C ₁₀ H ₁₈ O ₄	Octanedioic acid, dimethyl ester	
	14.30	74,87,43,41,55	214	C ₁₃ H ₂₆ O ₂	Dodecanoic acid, methyl ester	
	14.57	55,83,74,152,111	216	C ₁₁ H ₂₀ O ₄	Nonanedioic acid, dimethyl ester (azelaic acid methyl ester)	

15.32	74, 87,43,41,55	228	C ₁₄ H ₂₈ O ₂	Tridecanoic acid, methyl ester*
15.60	74,55,125,98,97	230	C ₁₂ H ₂₂ O ₄	Decanedioic acid, dimethyl ester †
17.16	74,87,43,55,143	256	C ₁₆ H ₃₂ O ₂	Pentadecanoic acid, methyl ester
18.00	74,87,43,55,41	270	C ₁₇ H ₃₄ O ₂	Hexadecanoic acid, methyl ester (Palmitic acid, methyl ester)
18.87	74,87,143,41,129	284	C ₁₈ H ₃₆ O ₂	Heptadecanoic acid, methyl ester
19.61	74,87,43,55,41	298	C ₁₉ H ₃₈ O ₂	Octadecanoic acid, methyl ester (Stearic acid, methyl ester)
21.28	69,137,71,83,201	NA	NA	NA
21.60	74,87,43,55,57	340	C ₂₂ H ₄₄ O ₂	Heneicosanoic acid, methyl ester
23.72	74,87,43,55,57	382	C ₂₅ H ₅₀ O ₂	Tetracosanoic acid, methyl ester

712 * co-elution, † means that only a trace of compounds was detected

713